
Article:
Abbas, Q., Thomson, T., Hayward, T. et al. (1 more author) (2020) Influence of Ga evaporation rate on the magnetic properties of amorphous FeGaSiB thin films. Journal of Magnetism and Magnetic Materials, 498. 166160. ISSN 0304-8853

https://doi.org/10.1016/j.jmmm.2019.166160

Influence of Ga evaporation rate on the magnetic properties of Amorphous FeGaSiB thin films

Qayes A. Abbas[1, 2], Thomas Thomson[3], Thomas J Hayward[1], Nicola A. Morley[1*]

[1]Dept of Materials Science & Engineering, University of Sheffield, Sheffield, UK, S1 3JD.

[2]Dept of Phys, College of Science, University of Anbar, Anbar, Iraq.

[3]School of Computer Science, University of Manchester, Manchester, M13 9PL UK.

[*]Corresponding author: n.a.morley@sheffield.ac.uk

Abstract

In this study, amorphous FeGaSiB thin films have been fabricated on silicon (100) substrates using a co-sputtering-evaporation deposition system. By fixing the sputtering parameters (chamber pressure and power of the FeSiB target), and only varying the Ga evaporation rate, how the morphology, magnetic properties, and magnetostriction constants changed with the addition of Ga were investigated. This was to increase the Ga concentration, while maintaining the optimized fabrication parameters established in previous work. It was determined that the percentage of Ga increased linearly as the Ga evaporation rate was increased. The x-ray diffraction (XRD) results indicated that all the films were amorphous and the only detected peaks were for the Si substrate. The results showed that varying Ga evaporation rate, thus Ga content, affected the magnetic properties of the films by reducing the saturation induction along with increasing the uniaxial anisotropy within the films. The magnetostriction constants measured were in the range of 10.2 ppm to 17.2 ppm.

Keywords: Evaporation rate; Magnetostrictive; amorphous; uniaxial anisotropy.

1. Introduction

The potential of magnetostrictive amorphous materials, such as metallic glass, for micro-electro-mechanical systems (MEMS) [1][2] is well established. Amorphous Metglas FeSiB alloys in bulk [3] or ribbon [4][5] form are of interest for applications including transformer cores and variable-speed motors [6]. This is because FeSiB ribbon [7] with thickness 23 μm, magnetostriction constant 27 ppm, saturation field <1 kA/m, and magnetisation 1241 kA/m is useful for low core loss at high frequencies >1 kHz and can be used at high operating temperature with minimum flux density reduction. However, the MEMS applications, such as magnetic field sensors [8][9] require a large magnetostriction constant (λ_s > 20 ppm) and a small anisotropy field (H_k < 1 kA/m), plus are compatible with the MEMS fabrication processes. Therefore, FeSiB ribbon alloy does not achieve all these requirements. Thus, FeSiB in thin film form has become more interesting, with many studies carried out to investigate their soft magnetic properties, so that they can be used in applications such as low field sensors.

The effect of different deposition techniques such as r.f sputtering [10], thermal evaporation [11], co-sputtering [12] and growth parameters on the material properties have been studied to develop magnetostrictive thin films, including Fe-based films, such as amorphous FeSiB [10], and crystalline FeGa [13]. By improving the performance of these films, it will be possible to achieve the required properties for MEMS devices such as strain sensors [14] and actuators [2]. Previous research has studied crystalline FeGa thin films in thickness range 20 nm < t < 200 nm [15], by changing the growth parameters, for example, Javed *et al* [16] studied the effect of Ga evaporation rate and sputtering growth parameters on the Fe:Ga ratio and how these parameters effected the magnetic properties and effective magnetostriction constant, λ_{eff}, of $Fe_{100-x}Ga_x$ ($14 \leq x \leq 32$) thin films. These authors found that, for fixed Ar pressure and sputtering power, and varying Ga evaporation rate (0.2, 0.3 and 0.4 arbitrary units (a.u)), the films had a saturation fields of about 100 kA/m for $x \leq 15$ while it was constant at about 35 kA/m for $x \geq 15$. All the films had a nearly constant, λ_{eff} ~ 40 ppm for the Ga compositions investigated.

Another option for soft magnetostriction thin films is to produce amorphous films. This is achieved by the addition of Si and/or B to transition metal elements. This is because removing the magnetocrystaline anisotropy improves the soft magnetic properties of the films, therefore making them candidates for MEMS applications [8].

For example, Kobliska *et al*. [17] studied six different types of amorphous thin films ($Co_{79}Fe_5B_{14}Mo_2$, $Fe_{73}B_{27}$, $Fe_{66}Cr_9B_{25}$, $Fe_{70}Si_{30}$, $Fe_{73}Si_6B_{21}$, $Fe_{62}Si_{19}B_{19}$) grown by rf sputtering at room temperature. The films were fabricated in the thickness range 300-500 nm, and the magnetic properties and magnetostriction constants were determined. They found, that the amorphous $Fe_{73}Si_6B_{21}$ film had a saturation magnetisation 955 kA/m, coercive field 15.9 A/m, saturation field 477 A/m, and magnetostriction constant 26 ppm, while the amorphous $Co_{79}Fe_5B_{14}Mo_2$ film had a maximum saturation magnetisation 1193 kA/m, low coercive field 3.97 A/m, saturation field 1432 A/m, and zero magnetostriction constant. This means $Co_{79}Fe_5B_{14}Mo_2$ film has the high magnetization and low coercive field required, but it does not have the high magnetostriction constant, while the Fe film has the high magnetostriction constant but lower magnetization. Therefore an ideal material would be a combination of the two.

Our previous work [18] on FeSiB and FeGaSiB thin films grown on Si substrate using a co-sputtering-evaporation technique determined how film thickness and sputtering pressure [19] affected the structural and magnetic properties. These results showed that adding Ga to amorphous FeSiB films in the thickness range 24–100 nm did not affect the morphology of the films, but the magnetic properties and magnetostriction constants were changed. We found that the addition of Ga, at Ga evaporation rate 0.2 a.u, into the FeSiB films decreased the saturation induction and changed the magnetic anisotropy from uniaxial to isotropic. For the FeGaSiB films, increasing the film thickness decreased the coercive field and increased the saturation field (H_s). For thicknesses ≥40 nm, the FeGaSiB magnetostriction constants were all larger than the FeSiB films magnetostriction constants. While changing the sputtering gas pressure at fixed Ga rate (0.2 a.u), for 50nm FeGaSiB film [19] did not affect the morphology of the films, but the magnetostriction constant decreased with increasing Ar pressure. This work extends our previous study, by using the optimised fabrication parameters (sputtering power (20W) and pressure (4 μbar)) determined from our previous papers [18, 19] and increasing the Ga concentration by increasing the Ga rate to investigate how a larger amount of Ga in the ratio FeSiB:Ga in these films, effects the morphology, magnetic properties, and magnetostriction constant (λ_s) of FeGaSiB thin films.

2. Experimental work

FeGaSiB thin films were fabricated on Si (100) substrates using a co-sputtering- evaporation

system [20]. Prior to deposition the 10mm x 15mm substrates were cleaned using acetone and isopropanol (IPA). The sputtering target used in this work was comprised of three layered sheets cut from 23µm Metglas 2605SA1 foil with nominal composition $Fe_{85}Si_{10}B_5$. A Ga ingot was used in the evaporator. FeGaSiB films of thickness 50 nm were deposited using growth parameters: sputtering power (P_{FeSiB}) of 20W, Ar pressure 4µbar, the substrate-target distance (d) 60 mm, and the Ga evaporated at different rates R_{Ga} = (0.2, 0.3, 0.4, 0.5, and 0.6 a.u.), controlled by a rate monitor. For each film, the evaporation power was varied to maintain the rate during growth. Rotating the substrate holder during the deposition was necessary to remove the influence of the sputter gun magnetron field, which can produce magnetic anisotropy within the films and also ensured an even distribution of the Ga within the films. A magneto-optical Kerr effect (MOKE) magnetometer was used, in transverse mode to measure the film's magnetic properties at room temperature. The maximum applied magnetic field was 40 kA/m, which was sufficient to ensure saturation of the films' magnetisation. The normalized magnetization hysteresis loops were measured as a function of applied magnetic field direction with respect to one edge of the film (designated as angle 0º), between angles 0° to 180°. This allowed the in-plane magnetic anisotropy, induced by growth parameters, to be determined. At room temperature, the magnetostriction constants (λ_s) [15] were measured using the Villari effect technique [14],[21]. This involved straining the films over several different bending radii while recording the corresponding hard-axis hysteresis loop using MOKE. By using the method described in Ref. [22], the value of H_k was determined. Then H_k was plotted against of the bending radii ($1/R$), and the magnetostriction constants (λ_s) were calculated from [15], [22].

$$\lambda_S = \frac{d(H_k)}{d\left(\frac{1}{R}\right)}\left\{\frac{2\mu_o M_s\left(1-v^2\right)}{3tE}\right\} \quad (1)$$

Where H_k is the anisotropy field, the bending radii were R=300, 400 and 500 mm, μ_o is the permeability of space, M_s is the saturation magnetization of the film, E is the Young's Modulus of silicon substrate (E=130 GPa), t is the thickness of the silicon substrate (t =380 µm) and ν is the Poisson ration of silicon substrate (ν =0.28).

X-Ray diffraction (XRD) measurements were undertaken using a Bruker D2 phaser with a Cu $K_{\alpha 1}$ (wavelength =1.54184 Å) source to examine the structure of the films. In the θ/2θ geometry, two separate measurements were made; the first was for the 2θ in range from 30º to

80° to study the structure of the films and substrate (for bcc Fe 2θ <110> = 44.61° and for bcc Fe-Ga 2θ <110> = 44.29° (10%Ga) to 43.81° (25%Ga) [23] and for the silicon substrate (peaks at 2θ = 69°, 61.7°, and 33°)). The second was for 2θ in range from 35° to 55° to avoid the above-mentioned Si substrate peaks allowing for more detailed scan of the magnetic films, which is normally dwarfed by the highest Si peak intensity. A DMS model 10 vector vibrating sample magnetometer (VSM) was used to determine the magnetic moment of the films at room temperature, using applied field of 40 kA/m, from which the saturation magnetisation was calculated. X-ray photoelectron spectroscopy (XPS) was performed on a Thermo Fisher Scientific K-alpha+ spectrometer to determine the composition of the films. Samples were analyzed using a micro-focused monochromatic Al x-ray source (72 W) over an area of approximately 400 µm. Data was recorded at pass energies of 150 eV for survey scans and 40 eV for high resolution scan with 1 eV and 0.1 eV step sizes respectively. Charge neutralization of the sample was achieved using a combination of both low energy electrons and Argon ions. Initial analysis of the samples revealed high levels of carbon attenuating the underlaying metallic elements. To minimize this contamination all samples were cleaned with argon clusters of approximately 2000 atoms, from a Thermo MAGCIS source operating at 4 kV and raster over a 2 mm^2 area for a period of 30 seconds. Data analysis was performed in CasaXPS using a Shirley type background and Scofield cross sections, with an energy dependence of -0.6.

3. Result & discussion

3.1 XRD result and XPS measurements

XRD measurements were taken to examine whether the films were completely amorphous or if they included crystalline clusters in an amorphous matrix.

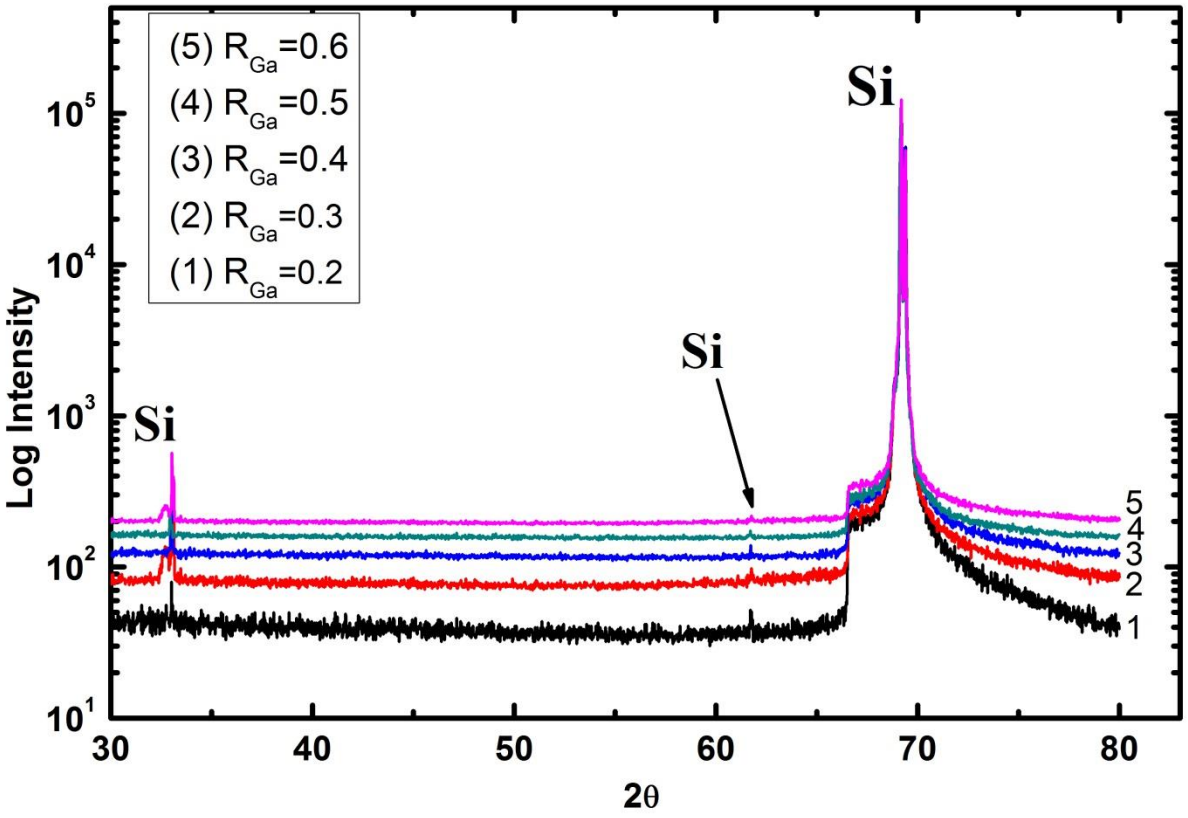

Figure 1 XRD result of FeGaSiB thin films with different Ga evaporation rates.

Figure 1 shows the XRD patterns of FeGaSiB films with varying Ga evaporation rates. The log intensity scale was used to enhance the visibility of small peaks, which are small in size relative to the highest intensity of the Si substrate. It shows that all the films had an amorphous structure and all the peaks present were for the Si substrate. It can be seen from the figure there are no peaks existing at $2\theta \sim 45^{o}$, which would be expected if crystalline Fe or the Fe-Ga (110) texture were present within the films [24]. Hence the films had an amorphous structure. Thus Figure 1 shows that varying the Ga evaporation rate does not influence the film morphology, so it is independent of the amount of Ga in the films.

Table 1 the XPS result of the film's composition via the Ga evaporation rate.

Ga evaporation rate	**Fe %conc**	**Ga %conc**	**Si %conc**	**B %conc**
0.2	82	7	5	6
0.3	83	8	4	5
0.4	79	11	5	5
0.5	79	12	5	4
0.6	77	14	5	4

Figure 2(a) shows the XPS spectra for the Si(2s), Ga(3s) and B(1s) peaks. It is observed as a function of Ga rate, the Ga(3s) peak area increases, while for the Si(2s) and the B(1s) peaks it is not possible to visually see any changes in area as the Ga rate increases. Using the CasaXPS fitting programme, for each film the %concentration (%conc) for each element was determined, and are given in Table 1. The results showed that Ga was successfully added to FeSiB films by using the co-sputtering-evaporation technique, to fabricate the FeGaSiB films. For fixed pressure and power, the results show that increasing the Ga evaporation rate led to an increase in the Ga concentration. Thus allows for control of the Ga percentage within the films. It can be seen in Figure 2(b) that the composition of Ga has a linear relation with Ga evaporation rate (R_{Ga}). Thus the Ga composition can be controlled over a range of 7% by changing the Ga evaporation rate (R_{Ga}), whilst maintaining all the remaining fabrication parameters constant. The data in table 1 also show that the Fe and B concentrations decrease with Ga concentration increase. While the Si concentration is maintained within the accuracy of the measurement.

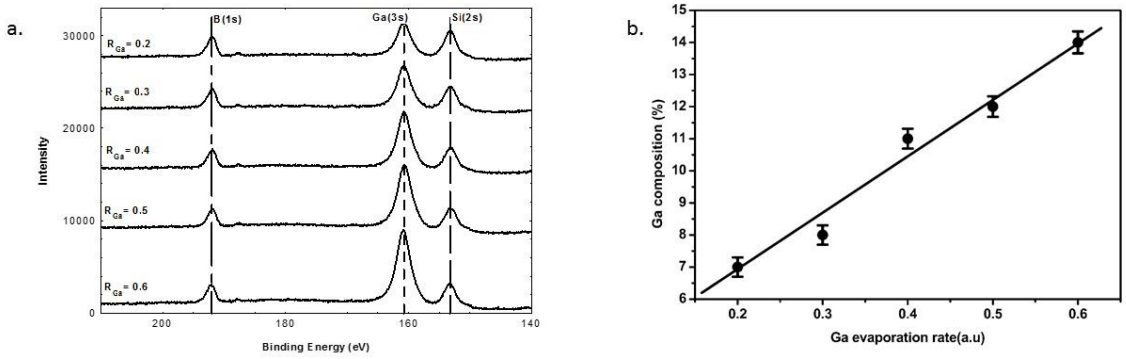

Figure 2(a). XPS spectra for the Si(2s), Ga(3s) and B(1s) for the different FeGaSiB films. The data has been off set along the y axis. 2(b). Ga composition as a function of Ga evaporation rate under constant pressure 4μbar and power 20W. The solid line is a guide for the eye.

3.2 Magnetic properties

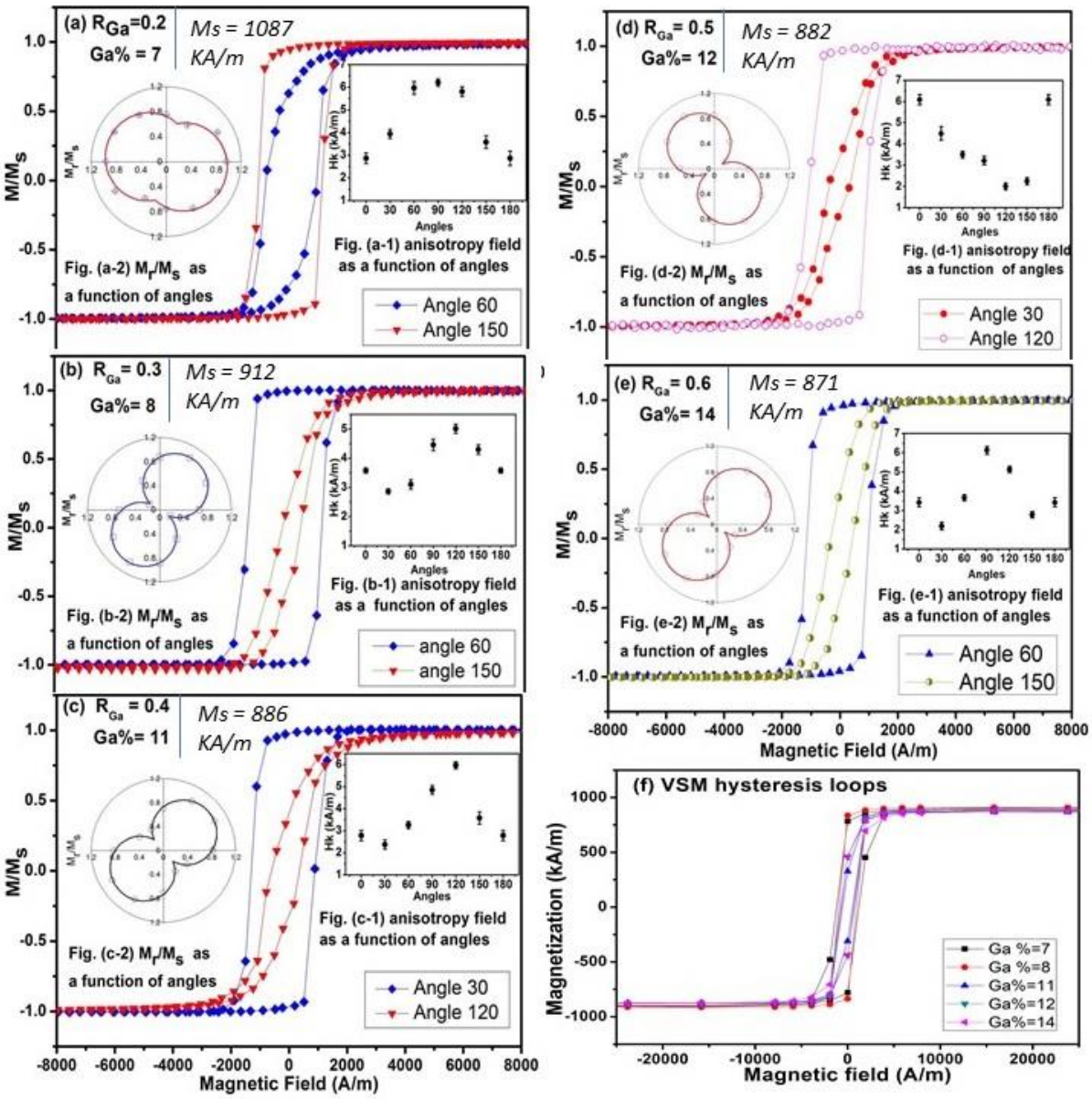

Figure 3(a-e) The hard and easy normalized hysteresis loops of FeGaSiB films for Ga percentages. The insert figures refer to the anisotropy fields (right side) and the angular plot of the remanence ratio (M_r/M_s) (left side). The lines are a fit to the data. 3(f) Magnetisation as a function of magnetic field taken on a VSM for all the samples. All the loops were taken at

room temperature.

Figures 3(a, b, c, d, and e) shows the hard and easy normalized hysteresis loops for the unstrained FeGaSiB films, where the anisotropy fields were determined as a function of the angle between the applied magnetic field and edge the film. The insert figures refer to the anisotropy fields (right side) and the angular plot of the remanence ratio (M_r/M_s) (left side). There are two methods of quantifying the uniaxial anisotropy of a material. The first method involves determining the anisotropy constant from the anisotropy field using the following equation.

$$K = \frac{\mu_o H_k M_s}{2} \tag{2}$$

Where K is the anisotropy constant, H_k is the anisotropy field, M_s is the saturation magnetization, and μ_o is the permeability of space.

The second method to quantified the uniaxial anisotropy involves fitting eqn (3) for M_r/M_s as a function of angle to the data [25] as shown in Figure 3 (insert left figures):

$$\frac{M_r}{M_S} = D|cos\ (\theta - \theta_o)| + c \tag{3}$$

Where D refers to the strength of the uniaxial anisotropy, θ is referring to the angle between the easy axis and the field, θ_o is referring to the angle between the easy axis and the side of the film, c is the lowest measured $\frac{M_r}{M_S}$. For an isotropic film, $D = 0$, as M_r/M_s is a constant, while for $D < 0.5$, the anisotropy within the film is weakly uniaxial and for $D > 0.5$, the anisotropy is strongly uniaxial. Thus for the film at Ga 7%, D ≈ 0.3, so has weak uniaxial anisotropy, while a stronger uniaxial anisotropy is present in the film at Ga 8% where D ≈ 0.83 (see Figure 4).

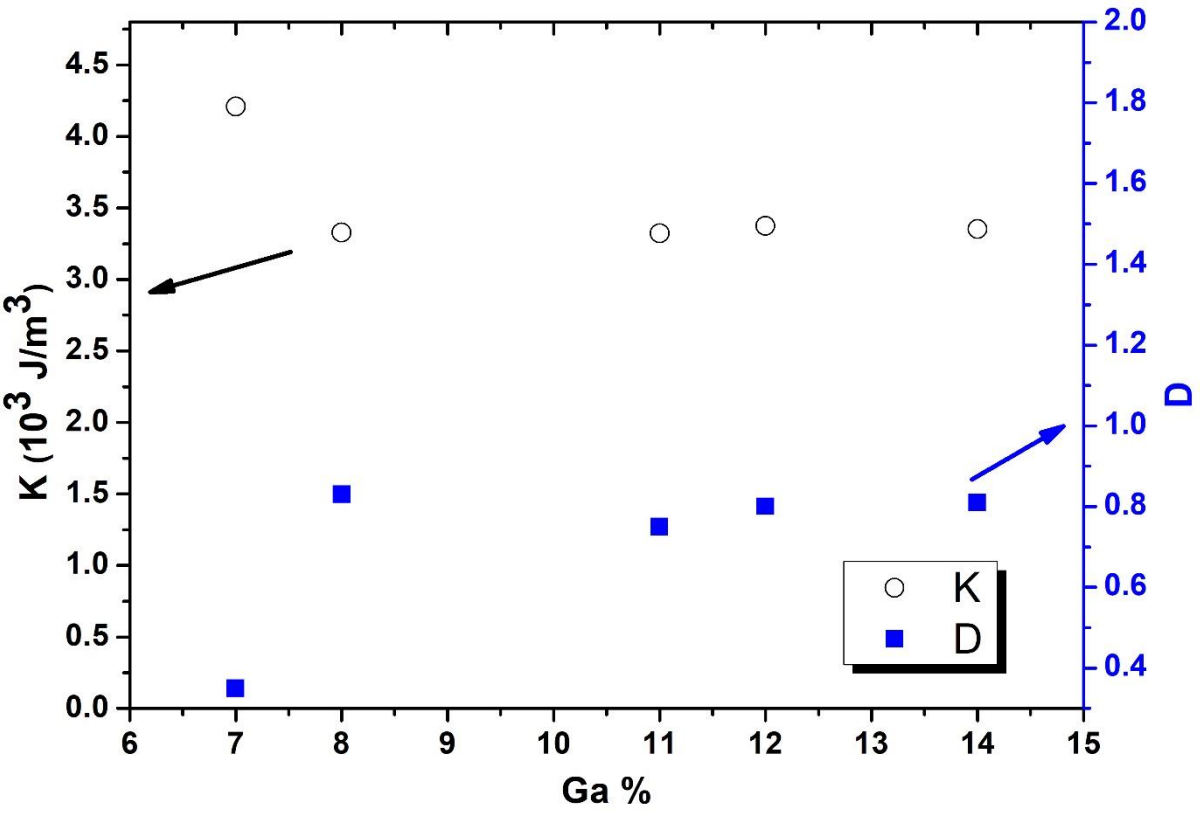

Figure 4 Anisotropy constant (K) and the strength of uniaxial anisotropy (D) as a function of Ga concentrations.

Figure 4 shows the anisotropy constant *(K)* and the strength of uniaxial anisotropy *(D)* as a function of Ga concentrations. From Figure 4, it is observed that the two quantifiers show that for Ga concentration above 8%, the uniaxial anisotropy is the same for all the films independent of Ga concentration, as $K \sim 3.3$ kJm^{-3} and $D \sim 0.8$ for all the films. While the 7% Ga film had the largest anisotropy constant and the smallest *D*, which means the two methods give contradiction results, this is discussed below.

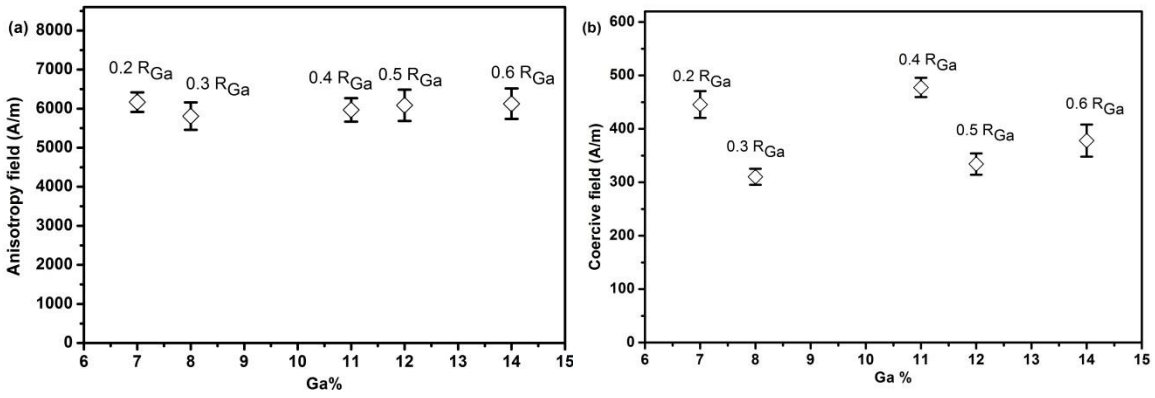

Figure 5 (a) Anisotropy field and (b) Coercive fields as a function of Ga concentration rate for FeGaSiB thin films

From Figure 5 (a), for all the films (Ga% from 7% to 14%), $H_k \approx 6000$ A/m, as derived from the hard axis loops. The anisotropy field was determined from the hard axis normalized MOKE loops as the field at which M/M_s equals ±1. This shows that even with the increase of Ga within the films, the anisotropy field was maintained. Comparing the anisotropy fields to a 50nm FeSiB film grown with the same fabrication parameters and $H_k \approx 2300$ A/m [18,19], the FeGaSiB films all have a higher anisotropy field. The anisotropy energy depends on the anisotropy constant, which is given by eqn (2). From Figure 6, it is observed that there is a decrease in M_s with increase in Ga concentration. Thus the anisotropy constant of 7% Ga films is $K = 4210$ Jm^{-3}, while the 14% Ga film is $K = 3352$ Jm^{-3} (Figure 4). Thus suggests that the uniaxial anisotropy energy in the 7% Ga film is the largest, while from Figure 4, it has the smallest D, suggesting it has the smallest uniaxial anisotropy. The reason for this is that the two methods use different parameters from the magnetic hysteresis loop. The remnant magnetization is expected to at least partially depend on the pinning of domain walls in the film close to zero field, while the anisotropy field is primarily determined by the strength of the film's anisotropy energy, which will work to prevent magnetization rotation at higher field strengths. Thus, the 14% Ga film, has less pinning compared to the 7% Ga film, so a smaller M_r/M_s along the hard axis, this leads to the observation of strong uniaxial anisotropy observed in Figure 3 inset, but as it has a smaller M_s compared to the 7% Ga film but the same H_k, so the anisotropy constant, hence energy is smaller compared to the 7% Ga film.

Figure 5(b) shows the coercive field, along the hard axis loop, as a function of the Ga concentration for the FeGaSiB thin films. The coercive fields were in the range from (300 to 500) A/m, which are lower than the coercive field of a 50nm FeSiB film, grown with the same fabrication parameters [18, 19] of $H_c \approx 800$ A/m. This means that the Ga addition has reduced

the coercive field, probably due to reduced domain wall pinning in the higher concentration films, as suggested by the Mr/M_s data.

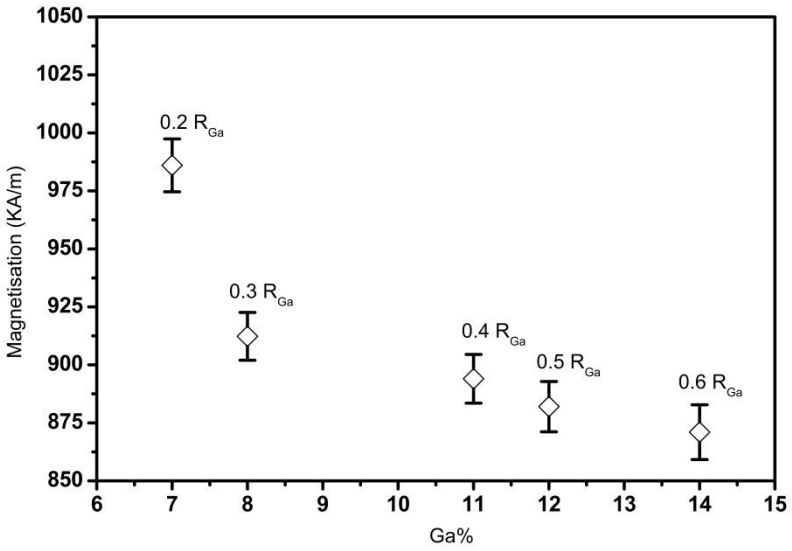

Figure 6 Saturation magnetisation as a function of Ga % of FeGaSiB thin film.

Figure 6 shows the saturation magnetization for FeGaSiB thin films measured by the VSM technique at room temperature, taken from the hysteresis loops in Figure 3(f). From Figure 6, it is noted that the magnetization of the films reduces with increasing the Ga evaporation rate, hence the Ga concentration, and consequent decreasing Fe concentration (Table 1). As Ga is a non-magnetic element, it will decrease the magnetization of the films, along with changing the distribution of Fe atoms within the films, which can produce a variation in the films' composition [26], [14]. This lead to a distribution of the non-magnetic different atoms in the local environment within the amorphous matrix, i.e. the nearest neighbours Fe atoms. As the magnetic moment of the Fe atoms is dependent directly on the nearest neighbours in the local environment, hence, the magnetization of the film will depend upon the atomic nearest neighbours. This is observed as the Fe drops by 5% across the films, while the magnetization drops by 13%. Hence the Ga does disrupt the Fe nearest neighbours to change the magnetization. In general changing the amorphous distribution presents fluctuations in the exchange interactions, which impact the magnetic properties of the material. For example, the saturation magnetization of composition $Nd_2Fe_{11.5-x}Co_{2.5}Ga_xB$ decreases with increasing Ga content, as Ga is a non-magnetic element and will occupy certain the Fe sites, so changing the contribution of the Fe atoms [27].

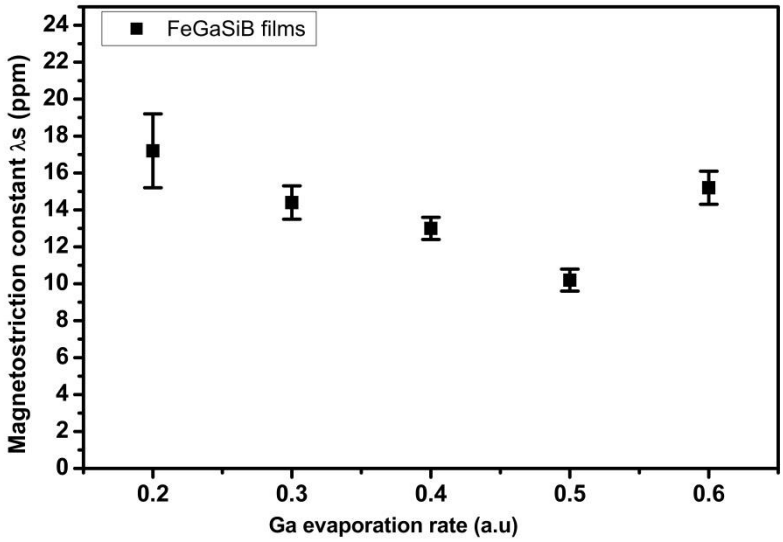

Figure 7 Magnetostriction constant as a function of Ga evaporation rate of FeGaSiB thin film.

From Figure 7 it is observed that the magnetostriction constants of FeGaSiB thin films decrease with increasing of the Ga evaporation rate until R_{Ga} = 0.5 (Ga% =12), then increased for R_{Ga} = 0.6 (Ga% =14). The films have the highest magnetostriction constants, λ_s, at the lowest Ga evaporation rate with the maximum λ_s = 17.2 ± 0.3 ppm, at R_{Ga} = 0.2 (Ga% =7). Compared with Ref. [28], for amorphous FeGaB films, they found that the addition of B into the bcc FeGa films in the range of B%: 0-21 changed the content of Ga from 9 to 17% and the maximum value of the magnetostriction constant found to be 70 ppm at Boron content of 12at %. Further, Kobliska *et al* [17] found that the magnetostriction constant of amorphous films such as $Fe_{73}Si_6B_{21}$ had a saturation magnetostriction constant about 26 ppm, which is higher that the FeGaSiB films in our study, while the amorphous $Fe_{62}Si_{19}B_{19}$ films had saturation magnetostriction constant of 14 ppm, which is lower than FeGaSiB films. The minimum value for FeGaSiB films was λ_s = 10.2 ± 0.3 ppm at R_{Ga} = 0.5 (Ga% = 12 and boron content 4 %) compared with Ref. [28] for the FeGaB films, which had a minimum magnetostriction constant of about 46 ppm at the Ga content 17 at% and B content 21at%. It would seem that the Ga and B percentage in the films are important for the magnetostriction constant. In addition, it was found that the FeGaSiB films minimum λ_s is higher that the amorphous $Co_{79}Fe_5B_{14}Mo_2$ film, which has a magnetostriction constant equal to zero [17]. This nonlinear behaviour of magnetostriction constant as a function of nonmagnetic element's contents was also observed in other amorphous magnetic structures such as FeCoB [29]. According to Ref. [30] the reason for magnetostriction nonlinear behaviour is due to a low amount of metalloid atoms such as

Boron leading to creation of atomic pairs, for example B-B and Ga-Ga that influence the magnetostriction behaviour. They suggest that increasing the content of metalloid atoms would lead to the formation of clusters that reduce the magnetostriction constant. Increasing the Ga evaporation rate from 0.2 to 0.6 increased the Ga percentage within the films from 7% to 14%, leading to changes in the local environment around the Fe atoms, hence changing the magnetic configuration and the exchange interaction of the Fe magnetic moments (Figure 6). This can also affects the stress within the films due to change the distribution of Fe and Ga atoms in an amorphous matrix, which is the probable reason why the strength of the uniaxial anisotropy increased in the films with higher Ga%. Thus, the magnetostriction constant, λ_s, is affected by saturation magnetization (Figure 6 and equation 1), depends on the composition and the stress presented within the films.

Conclusion

Fabrication of FeGaSiB films with different Ga evaporation rates did not change the film morphology as all the films were amorphous. Increasing the Ga evaporation rate, R_{Ga}, from 0.2 to 0.6 increased the concentration of Ga atoms from 7% to 14%. The addition of Ga atoms into the FeSiB films changed the strength of the uniaxial anisotropy present. The FeGaSiB films' magnetization decreased as the R_{Ga} increased, due to the nonmagnetic behaviour of Ga and replacing the other elements within the amorphous films and affected the local Fe environment. The magnetostriction constants reached a maximum value ≈17 ppm, for the $Fe_{82}Ga_7Si_5B_6$ film. Compared to a 50nm FeSiB film, the FeSiGaB films had softer properties, and similar magnetostriction constants, so would make an alternative thin film for MEMS applications.

Acknowledgements

We like to acknowledge the Iraqi Ministry of Higher Education & Scientific Research (MOHESR) for the financial support of this work and we like to acknowledge Dr. David Morgan and the XPS data collection was performed at the EPSRC National Facility for XPS ('HarwellXPS'), operated by Cardiff University and UCL, under contract No. PR16195.

References

[1] M. R. J. Gibbs, “Materials Optimization for Magnetic MEMS,” *IEEE Trans. Magn.*, vol. 43, no. 6, p. 2666, 2007.

[2] O. Cugat, J. Delamare, and G. Reyne, “Magnetic Micro-Actuators and Systems (MAGMAS),” *IEEE Trans. Magn.*, vol. 39, no. 6, pp. 3607–3612, 2003.

[3] J. M. Cadogan, S. J. Campbell, J. JingC. P. Foley, P. Kater, Y. W. Mai, “Annealing embrittlement of Fe_{78} Si_9 B_{13} (Metglas-2605S2 *),*” *Hyperfine Interactions*, vol. 13, pp. 7–14, 2014.

[4] M. Brouha, and J. Van Der Borst, “The effect of annealing conditions on the magneto - mechanical properties of Fe - B - Si amorphous ribbons the effect of annealing conditions on the magneto- mechanical properties of Fe-B-Si amorphous ribbons,” *Journal of Applied Physics*, vol. 7594, no. 1979, pp. 1–4, 2016.

[5] T. U. B. Itak, “Magnetic Domain Structures in As-Quenched and Annealed Fe_{78} B_{13} Si_9 Metallic Glass Ribbons,” *Turkish Journal of Physics,* vol. 22, pp. 481–488, 1998.

[6] R. Hasegawa, “Applications of amorphous magnetic alloys,” *Mater. Sci. Eng. A*, vol. 375–377, no. 1–2 SPEC. ISS., pp. 90–97, 2004.

[7] R. Hasegawa, “Advances in amorphous and nanocrystalline magnetic materials,” *Journal of Magnetism and Magnetic materials*, vol. 304, pp. 187–191, 2006.

[8] D. Viehland, M. Wuttig, J. McCord and E. Quandt, "Magnetoelectric magnetic field sensors", MRS Bulletin, vol. 43, no 11 pp. 834-840 2018.

[9] A. K. George, S. H. Al-harthi, R. V Ramanujan, and M. R. Anantharaman, “Metglas thin film based magnetostrictive transducers for use in long period fibre grating sensors,” *Sensors Actuators A. Phys.*, vol. 161 pp. 4–11, 2010.

[10] Z. G. Sun, H. Kuramochi, M. Mizuguchi, F. Takano, Y. Semba, and H. Akinaga, “Magnetic properties and domain structures of FeSiB thin films prepared by RF-sputtering method,” *J. Magn. Magn. Mater.*, vol. 272–276, pp. 1160–1161, 2004.

[11] M. Satalkar, S. N. Kane, A. Pasko, A. Apolinário, C. T. Sousa, J. Ventura, J. J. Belo, J. M. Teixeira, J. P. Araujo, F. Mazaleyrat, and E. Fleury, “Preparation and characterization of Fe-Si-B thin films,” *AIP Conf. Proc*., vol. 1512, pp. 654–655, 2013.

[12] J. R. Hattrick-Simpers, D. Hunter, C. M. Craciunescu, K. S. Jang, M. Murakami, J. Cullen,

M. Wuttig, I. Takeuchi, S. E. Lofland, L. Benderksy, N. Woo, R. B. Van Dover, T. Takahashi, and Y. Furuya, “Combinatorial investigation of magnetostriction in Fe-Ga and Fe-Ga-Al,” *Appl. Phys. Lett*., vol. 93, no. 10, pp. 10–13, 2008.

[13] J. Atulasimha and A. B Flatau. " A review of magnetostrictive iron–gallium alloys". *Smart Mater. Struct.* vol. 20, p. 043001, 2011.

[14] J.W. Judy, “Microelectromechanical systems (MEMS): fabrication ,and design”, *Smart Mater. Struct*. vol.10, pp. 1115–1134, 2001.

[15] A. Javed, N. A. Morley, and M. R. J. Gibbs, “Thickness dependence of magnetic and structural properties in Fe 80 Ga 20 thin films,” *Journal of Applied Physics,* vol. 107, p. 09A944, 2010.

[16] A. Javed, T. Szumiata, N. A. Morley, and M. R. J. Gibbs, “An investigation of the effect of structural order on magnetostriction and magnetic behavior of Fe–Ga alloy thin films,” *Acta Mater.*, vol. 58, no. 11, pp. 4003–4011, 2010.

[17] R. J. Kobliska, J. A. Aboaf, A. Gangulee, J. J. Cuomo, and E. Klokholm, “Amorphous ferromagnetic thin films,” *Appl. Phys. Lett.*, vol. 33, no. 5, pp. 473–475, 1978.

[18] Q. A. Abbas and N. A. Morley, “Fabrication and characterization of magnetostrictive amorphous FeGaSiB thin films,” *J. Magn. Magn. Mater.*, vol. 439, pp. 353–357, 2017.

[19] Q. A. Abbas, N. A. Morley, A. Johansson, and T. Thomson, “Influence of Ar Pressure on the Magnetic Properties of Amorphous FeGaSiB Thin Film*s*,” *IEEE Trans. Magn.*, vol. 53, no. 11, pp. 2–5, 2017.

[20] N. A. Morley, S. L. Yeh, S. Rigby, A. Javed, and M. R. J. Gibbs, “Development of a cosputter-evaporation chamber for Fe–Ga films,” *J. Vac. Sci. Technol. A*, vol. 26, no. 4, pp. 581–586, 2008.

[21] N. A. Morley, A. Javed, and M. R. J. Gibbs, “Effect of a forming field on the magnetic and structural properties of thin Fe-Ga films,” *J. Appl. Phys.*, vol. 105, no. 7, pp. 10–13, 2009.

[22] H. T. Savage and C. Adler, “Effects of magnetostriction in amorphous ferromagnets,” *Mater. Sci. Eng.*, vol. 99, no. 1–2, pp. 13–18, 1988.

[23] J. M. Borrego, J. S. Blázquez, C. F. Conde, A. Conde, and S. Roth, “Structural ordering

and magnetic properties of arc-melted FeGa alloys," *Intermetallics*, vol. 15, no. 2, pp. 193–200, 2007.

[24] B. W. Wang, S. Y. Li, Y. Zhou, W. M. Huang, and S. Y. Cao, "Structure , magnetic properties and magnetostriction of $Fe_{81}Ga_{19}$ thin film*s*," *Journal of Magnetism and Magnetic Materials*, vol. 320, pp. 769–773, 2008.

[25] E. Miskevich, F. K. Alshammari, W-G. Yang, J. Sharp, S. Baco, Z. Leong, Q. A. Abbas, N. A. Morley, "Artificial multiferroic structures using soft magnetostrictive bilayers on $Pb(Mg_{1/3}Nb_{2/3})$–$PbTiO_3$", *Journal of Physics D: Applied Physics*, vol. 51, pp. 085001, 2018.

[26] A. Javed, N. A. Morley, and M. R. J. Gibbs, "Structure, magnetic and magnetostrictive properties of as-deposited Fe-Ga thin films," *J. Magn. Magn. Mater.*, vol. 321, no. 18, pp. 2877–2882, 2009.

[27] J. Q. Xie, C. H. Wu, and Y. C. Chuang, "Effect of Gallium on The magnetic properties of $Nd_2Fe_{11.5}Co_{2.5}B$ compounds", *Solid state communications*, vol.71, no. 5, pp. 329-332, 1989.

[28] J. Lou, R. E. Insignares, Z. Cai, K. S. Ziemer, M. Liu, N. X. Sun, " Soft magnetism, magnetostriction, and microwave properties of FeGaB thin films", *Applied Physics Letters*, vol. 91, p.182504, 2007.

[29] L. P. Christopher, M. K. Minor, and J. K.Timothy, " Magnetic and Structural Properties of FeCoB Thin Films", *IEEE Transactions on Magnetics*, vol. 37, no. 4, p. 2302, 2001.

[30] E. Clark, M.Wun-Fogle, J. B. Restorff, T. A. Lograsso, and J. R. Cullen," Effect of Quenching on the Magnetostriction of $Fe_{1-x}Ga_x$ $(0.13< x < 0.21)$", *IEEE Transactions on Magnetics*, vol. 37, no. 4, p. 2678, 2001.